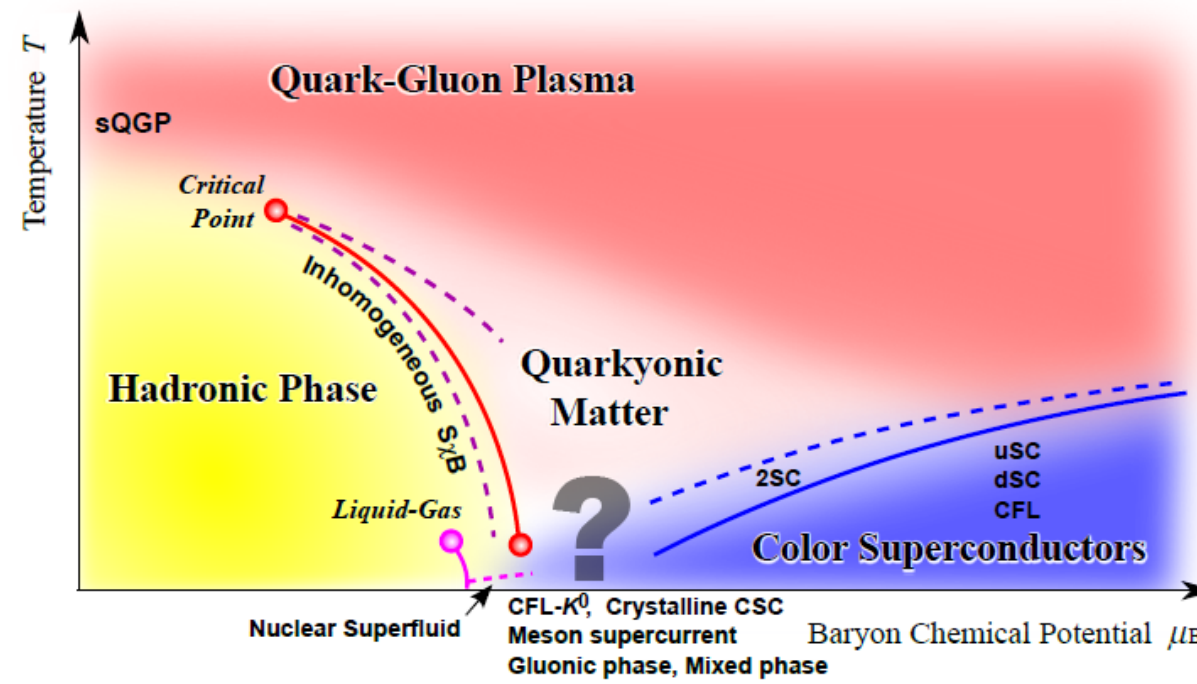


Magnetic susceptibility of strongly interacting matter

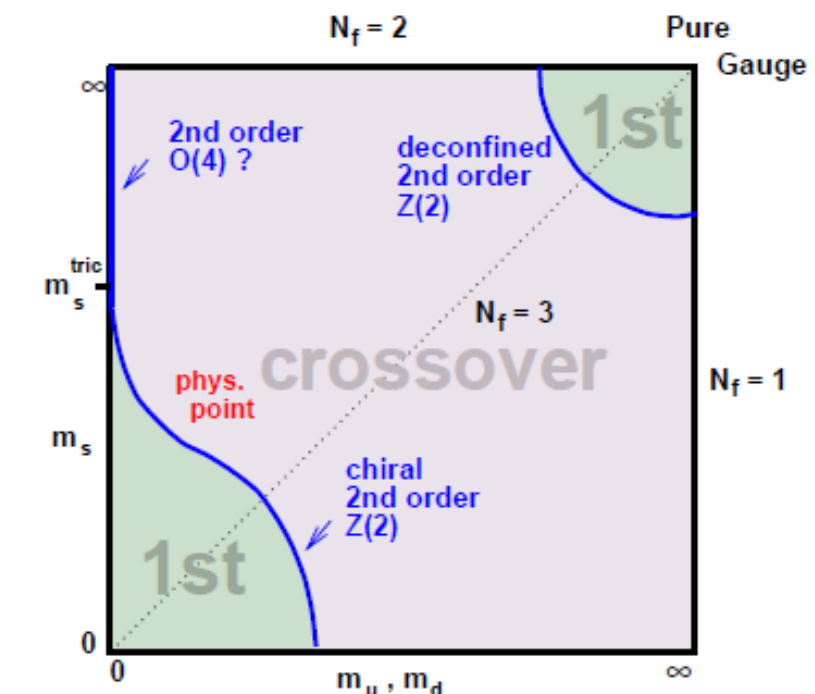
Kazuhiko Kamikado (RIKEN, Nishina center)
collaboration with
Takuya Kanazawa (RIKEN, iTHES)



QCD phase diagram



Fukushima et al., 1005.4814



Bonati et al., 1201.2769

- QCD shows rich phenomena when internal/external parameters are changed
 $T, \mu, N_c, N_f, m_u, m_s, \dots$
- External magnetic field is one of important parameters.
Magnetars : $10^{10} [T] = 10^6 [G]$
Non central heavy ion collision :
 $10^{11} [G] \sim eB = 0.1 [\text{GeV}^2] \sim 5 m_\pi^2$



Aim of this talk

- In this talk, we discuss properties of the strongly interacting matter under **static** magnetic field.
 - Magnetism of the QCD vacuum
 - Chiral phase transition under strong magnetic field



Free energy and χ

$$B^{ind} = B^{ext} + M = (1 + \chi)B^{ext}$$

Free energy: $\Omega = -P$

Magnetisation: $M = -\frac{\partial \Omega}{\partial(eB)} \sim \chi(eB)$

Magnetic susceptibility: χ

$$\Omega \sim \Omega_0 - \frac{\chi}{2}(eB)^2 + O(eB)^4 \quad \text{or} \quad P \sim P_0 + \frac{\chi}{2}(eB)^2 + O(eB^4)$$

- Magnetic susceptibility is the second order coefficient of the free energy.

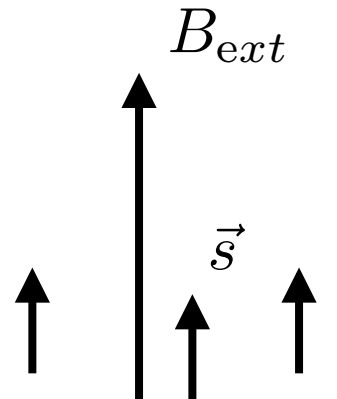


Electron gas (Landau vs Pauli)

$$B_{net} = (1 + \chi)B_{ext}$$

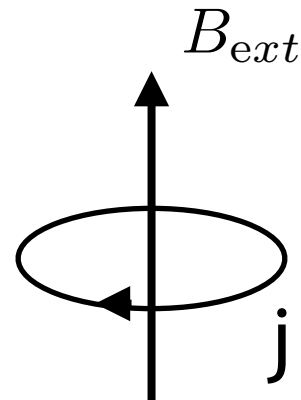
$$\chi_{\text{tot}} = \chi_{\text{spin}} + \chi_{\text{orbit}} > 0$$

Pauli paramagnetism (Spin)



$$\begin{aligned}\chi_{\text{spin}} &= 2\mu_B^2 \rho(\epsilon_f) \\ &= \frac{\mu_B^2 m k_f}{3\hbar^2 \pi^2}\end{aligned}$$

Landau diamagnetism (Orbit)



Landau, 1930

$$\chi_{\text{orbit}} = -\frac{1}{3}\chi_{\text{spin}}$$

- Competition of spin and orbital angular momentum
- Totally, electron gas is paramagnetic.
- Magnetism of QCD vacuum will be determined by the nature of charged quarks and mesons.



Free particle (vacuum)

$$\Omega_q = \text{Tr} \log[iD + m_q]$$

Andersen and Khan (2011)

$$x_f = \frac{m_q^2}{q_f B}$$

$$= \frac{N_c}{16\pi^2} \sum_f \left(\frac{\Lambda^2}{2|q_f B|} \right)^\epsilon \left[\left(\frac{2(q_f B)^2}{3} + m_q^4 \right) \left(\frac{1}{\epsilon} + 1 \right) - 8(q_f B)^2 \zeta^{(1,0)}(-1, x_f) - 2|q_f B|m_q^2 \log x_f + \mathcal{O}(\epsilon) \right]$$

$$\sim \# \frac{1}{\epsilon} (q_f B)^2 + \text{regular terms}$$

- The B square term has a divergence ($\epsilon > 0$).
- χ must be renormalised by the renormalisation of QED.
- To avoid the cutoff dependence, the following renormalisation condition is usually imposed in non-perturbative methods.

$$\chi(T = 0) = 0$$

Normalised pressure Bonati et.al 2013

$$\Delta P = (P(T, B) - P(T, 0)) - (P(0, B) - P(0, 0))$$

$$\sim \frac{\hat{\chi}(T)}{2} (eB)^2 = \frac{\chi(T) - \chi(0)}{2} (eB)^2$$



Free particle (thermal)

Quark ($s = 1/2$)

$$P_q^f = N_c \frac{|e_f B| T}{\pi^2} \sum_{n=0}^{\infty} \alpha_n \int_0^{\infty} dp \log \left(1 + e^{-\beta \sqrt{p^2 + m_q^2 + 2|e_f B| n}} \right)$$

$$\sim P_q^f(T) + \frac{\chi_q}{2}(T)(eB)^2$$

$$\begin{aligned}\hat{\chi}|_q &= -\frac{1}{3} \left(\frac{e_f}{e}\right)^2 \mathcal{G}_q^{(1)}(0) \\ &= \frac{N_c}{3\pi^2} \left(\frac{e_f}{e}\right)^2 \int_0^{\infty} dp \frac{1}{\sqrt{p^2 + m_q^2}} \frac{1}{e^{\beta \sqrt{p^2 + m_q^2}} + 1} > 0\end{aligned}$$

Meson ($s = 0$)

$$P_{\pi^\pm} = -\frac{|eB| T}{\pi^2} \sum_{n=0}^{\infty} \int_0^{\infty} dp \log \left(1 - e^{-\beta \sqrt{p^2 + m_\pi^2 + (2n+1)|eB|}} \right)$$

$$\sim P_{\pi^\pm}(T) + \frac{\chi_\pi}{2}(T)(eB)^2$$

$$\begin{aligned}\hat{\chi}|_{\pi^\pm} &= \frac{1}{12} \mathcal{G}_{\pi^\pm}^{(1)}(0) \\ &= -\frac{1}{12\pi^2} \int_0^{\infty} dp \frac{1}{\sqrt{p^2 + m_\pi^2}} \frac{1}{e^{\beta \sqrt{p^2 + m_\pi^2}} - 1} < 0\end{aligned}$$

- Quarks show paramagnetism ($\chi > 0$), while pions show the diamagnetism ($\chi < 0$).
- This may be understood as a competition of the orbital and spin magnetisation.
(cf. Pauli paramagnetism and Landau diamagnetism)
- Let's see effects of interaction and phase transition.

→ Analysis on the quark meson model



3-flavor Quark meson model

$$\mathcal{L} = \bar{\psi} \left[\not{d} + g \sum_{a=0}^8 T_a (\sigma_a + i\gamma_5 \pi_a) \right] \psi + \text{tr}[\partial_\mu \Sigma \partial_\mu \Sigma^\dagger] + U(\rho_1, \rho_2) - h_i \sigma_i - c_a \xi$$
$$\xi = \det \Sigma + \det \Sigma^\dagger, \quad \Sigma = \sum_{a=0}^8 T_a (\sigma_a + i\pi_a)$$

$$U(\rho_1, \rho_2) = a^{(1,0)} \rho_1 + \frac{a^{(2,0)}}{2} \rho_1^2 + a^{(0,1)} \rho_2 \quad \rho_1 = \text{tr} [\Sigma \Sigma^\dagger]$$
$$\rho_2 = \text{tr} \left[\Sigma \Sigma^\dagger - \frac{1}{3} \rho_1 \right]^2$$

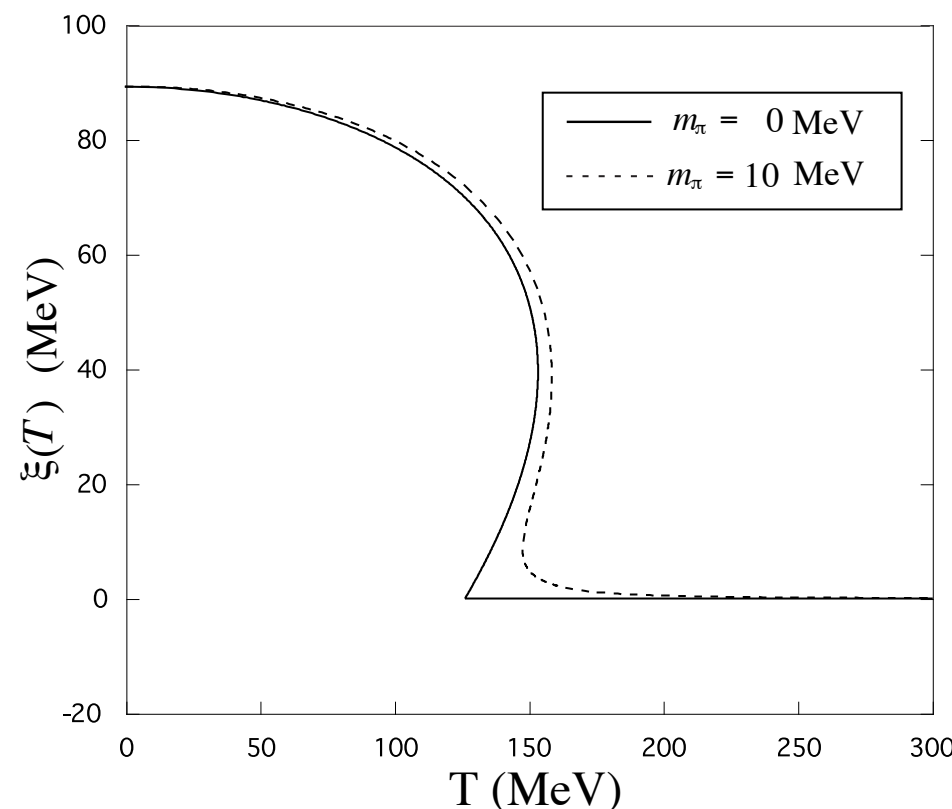
- Σ is 3x3 complex matrix i.e., composed of 8 scalar and 8 pseudo scalar mesons.
- ρ_1 and ρ_2 are invariants under the $U(3) \times U(3)$ flavour-chiral rotation.
- C_a is Kobayashi-Masukawa term which represents the effects of $U_A(1)$ anomaly.
- Inclusion of external magnetic field is achieve by

$$\partial_\mu \rightarrow D_\mu = \partial_\mu + ieA_\mu$$



Why Functional RG?

Perturbation theory at one-loop (O(4) scalar model)



S. Chiku and T. Hatsuda (1998)

$$\partial_\sigma U \Big|_{\sigma=\xi} = 0$$

- Meson fluctuation (at one-loop) makes phase transition first order.
(contrary to the universality argument [O(n) in 3d])
- We need Functional-RG as a machinery to include meson loops effectively.



Functional RG

$$k\partial_k \Gamma_k[\varphi] = \frac{1}{2} \text{Tr} \left[\frac{k\partial_k R_{kB}}{R_{kB} + \Gamma_k^{(0,2)}[\varphi]} \right] - \text{Tr} \left[\frac{k\partial_k R_{kF}}{R_{kF} + \Gamma_k^{(2,0)}[\varphi]} \right] \quad \underline{\text{C. Wetterich (1993)}}$$

Γ_k : scale dependent effective action

$$\begin{array}{ccc} \Gamma_{k=\Lambda}[\phi] = S[\phi] & \longrightarrow & \Gamma_{k=0}[\phi] = \Gamma[\phi] \\ \text{UV: classical} & & \text{IR: quantum} \end{array}$$

- Local potential approximation

$$\Gamma_k[\psi, \sigma, \pi] = \int_0^\beta dx_4 \int d^3x \left[\bar{\psi} [\gamma_\mu D_\mu + g(\Sigma + i\gamma_5 \Pi)] \psi + U_k(\rho_1, \rho_2) - h_i \sigma_i + ((D_\mu \Sigma)^2 + (D_\mu \Pi)^2) \right]$$

- Cut off choice (3d sharp cutoff)

$$R_{k,B}(q) = (k^2 - \vec{q}^2) \theta(k^2 - \vec{q}^2)$$

$$R_{k,F}(q) = -i\vec{p} \left(\frac{k}{|\vec{p}|} - 1 \right) \theta(k^2 - \vec{p}^2)$$



RG equation for U_k

$$\partial_k U_k = \frac{k^4}{12\pi^2} \left\{ \sum_{\pi, k, a, \phi, \sigma, \sigma', \eta, \eta'} \alpha_{e_b}(k) \frac{\coth \left[\frac{E_b}{2T} \right]}{E_b} - \sum_{u, d, s} \alpha_{e_f}(k) \frac{\tanh \left[\frac{E_f}{2T} \right]}{E_f} \right\} \quad \underline{\text{Skokov 2012}}$$

$$\alpha_{e_f}(k) = 6N_c \frac{e_f B}{k^2} \left(1 + 2 \sum_{n=1}^{\infty} \sqrt{1 - 2 \frac{e_f B}{k^2} n} \theta \left[1 - 2 \frac{e_f B}{k^2} n \right] \right) \rightarrow 4N_c (e_f B = 0)$$

$$\alpha_{e_b}(k) = 3 \frac{e_b B}{k^2} \sum_{n=0}^{\infty} \sqrt{1 - \frac{e_b B}{k^2} (2n+1)} \theta \left[1 - \frac{e_b B}{k^2} (2n+1) \right] \rightarrow 1 (e_b B = 0); .$$

Scale dependent Energies

M.Mitter and B. J .Shaefer 2013

$$E_{u,d}^2 = k^2 + \frac{g^2}{4} \sqrt{\frac{4\rho_1 - \sqrt{24\rho_2}}{3}} \quad E_{k,\pi}^2 = k^2 + \partial_{\rho_1} U_k + \sqrt{24\rho_2} \partial_{\rho_2} U_k - \frac{c_a}{2} \sqrt{\frac{4\rho_1 + 2\sqrt{24\rho_2}}{3}} \quad , \text{etc}$$

- Taylor expansion up to 3rd order ($i,j \leq 3$)

$$U_k(\rho_1, \rho_2) = \sum_{i,j} \frac{a_{i,j}}{i!j!} (\rho_1 - \rho_{10})^i (\rho_2 - \rho_{20})^j$$

- Pressure is

$$P = -a_{0,0}|_{k=0} + c\sigma_0 + c_a\xi_0 + \int_{\Lambda}^{\infty} dk \partial_k U_k^F|_{\rho_1=\rho_2=0}$$

T. Herbst, et al. (2010)

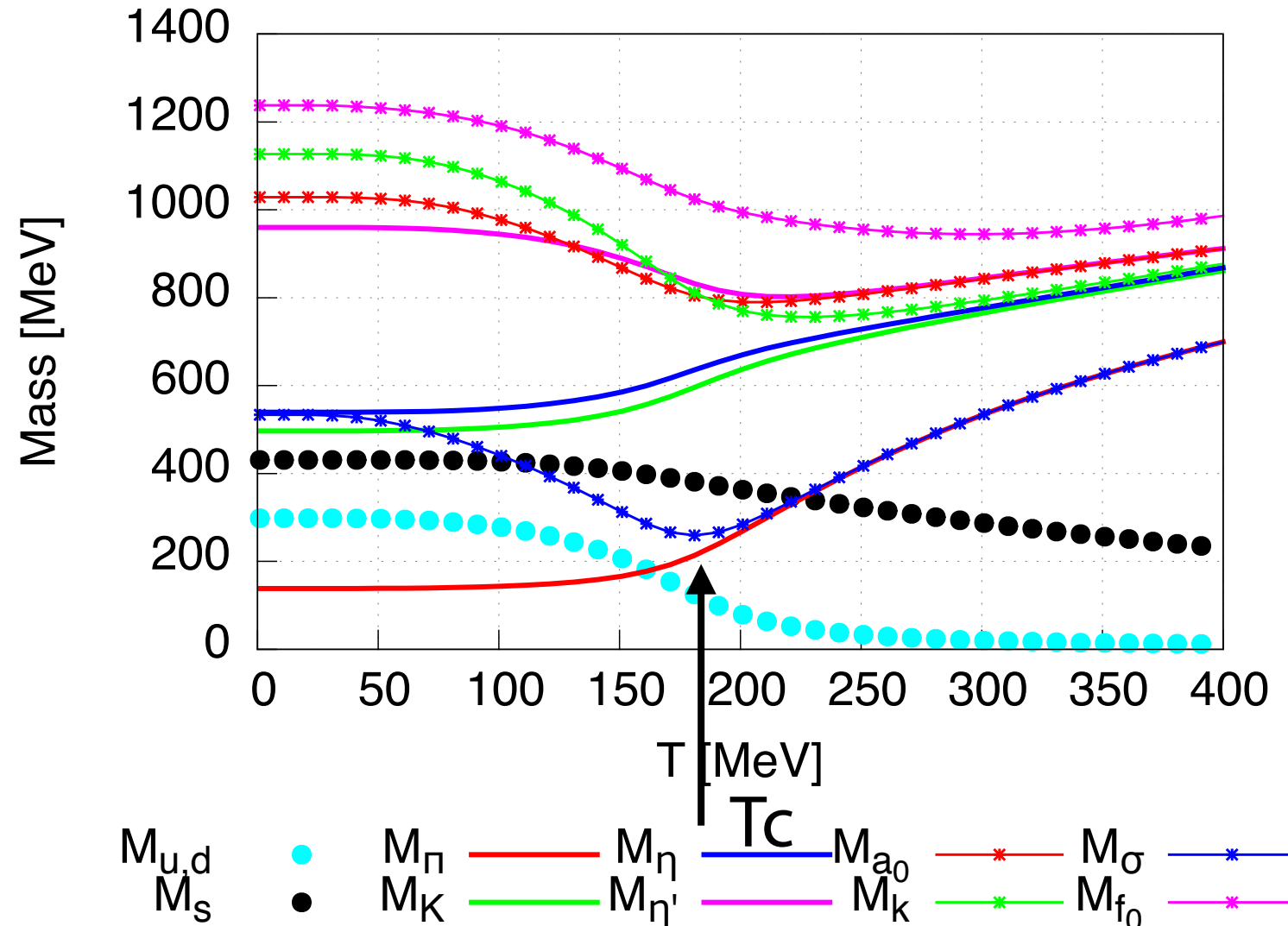


Numerical Results



Meson curvature masses

$$eB = 0$$

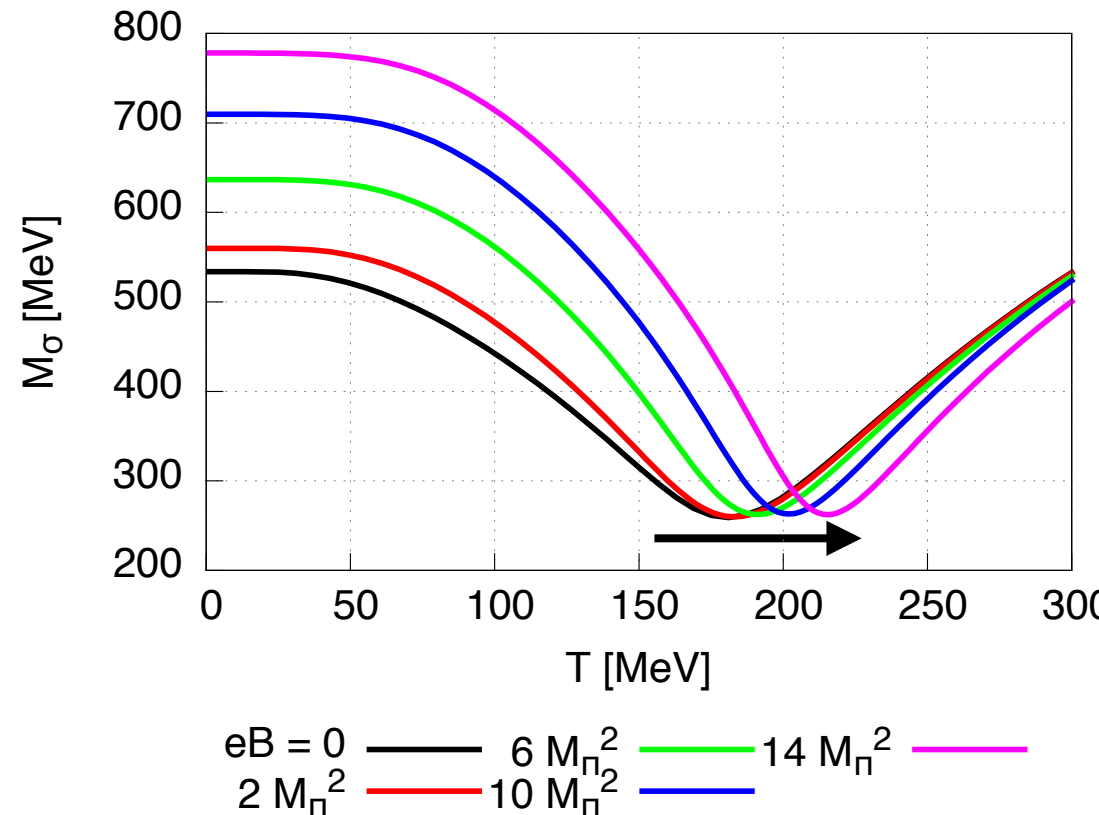


- Chiral phase transition occurs.
- T_c is determined by the minimum of sigma mass.

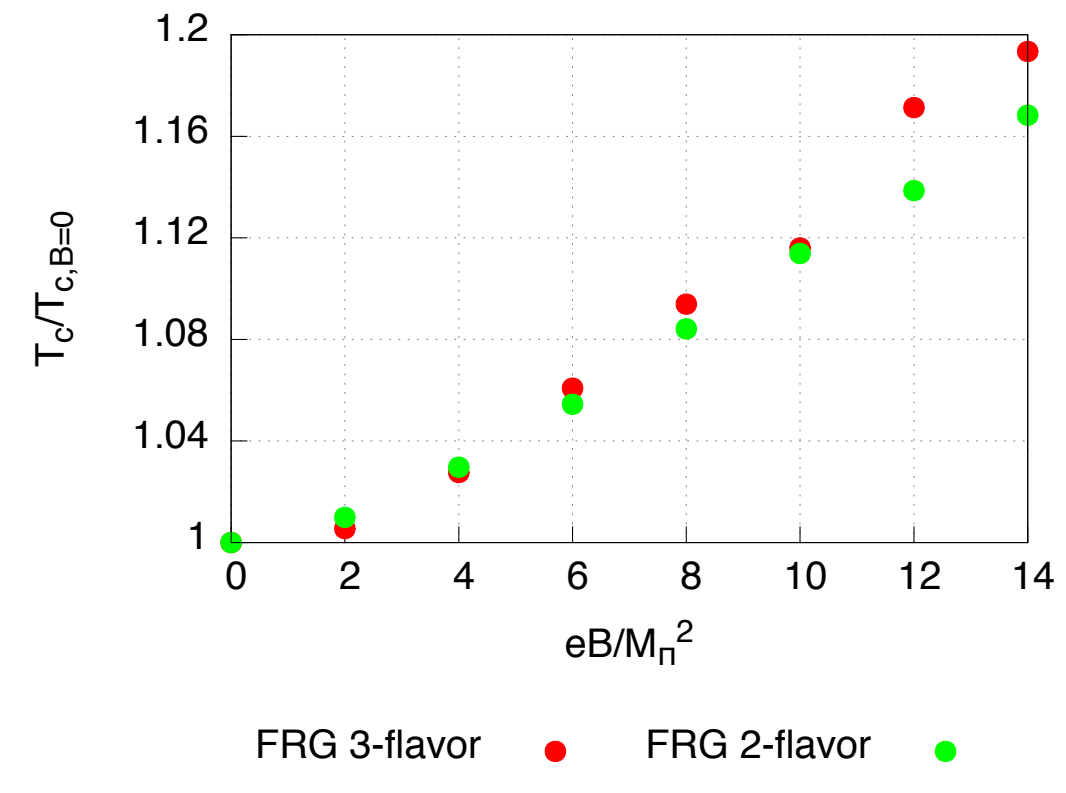


Phase transition

σ mass with varying eB



T_c at finite eB

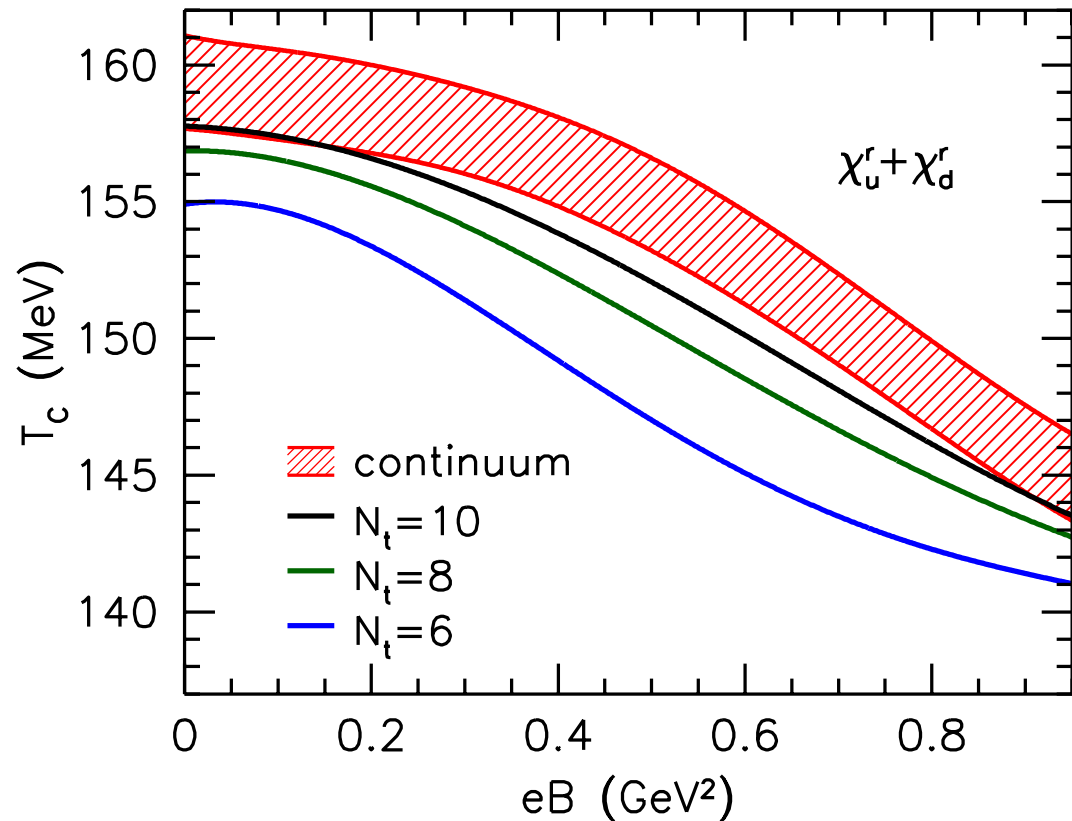


- T_c increases with increasing eB . (Magnetic catalyses)

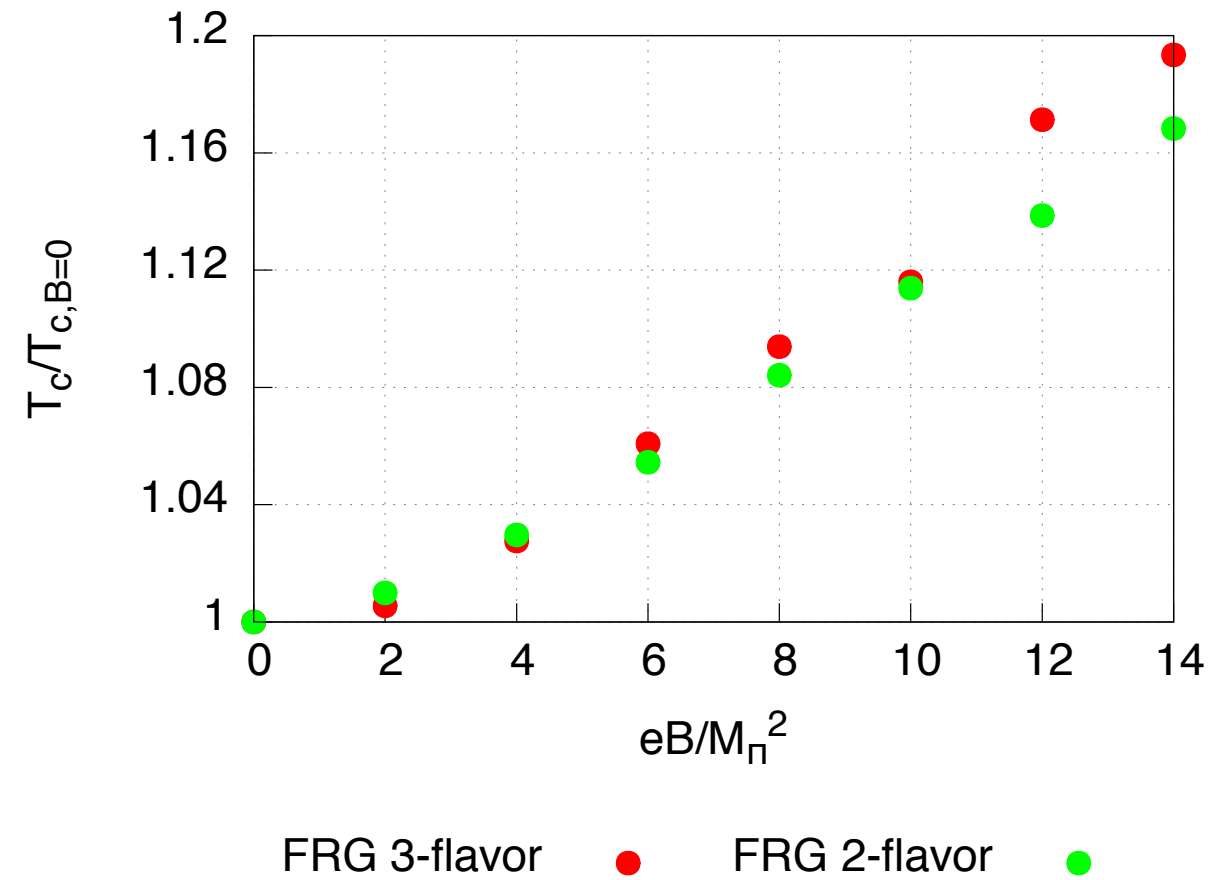


Anti-Magnetic catalyses

2+1 flavor Lattice [G.S. Bali et al. (2012)]



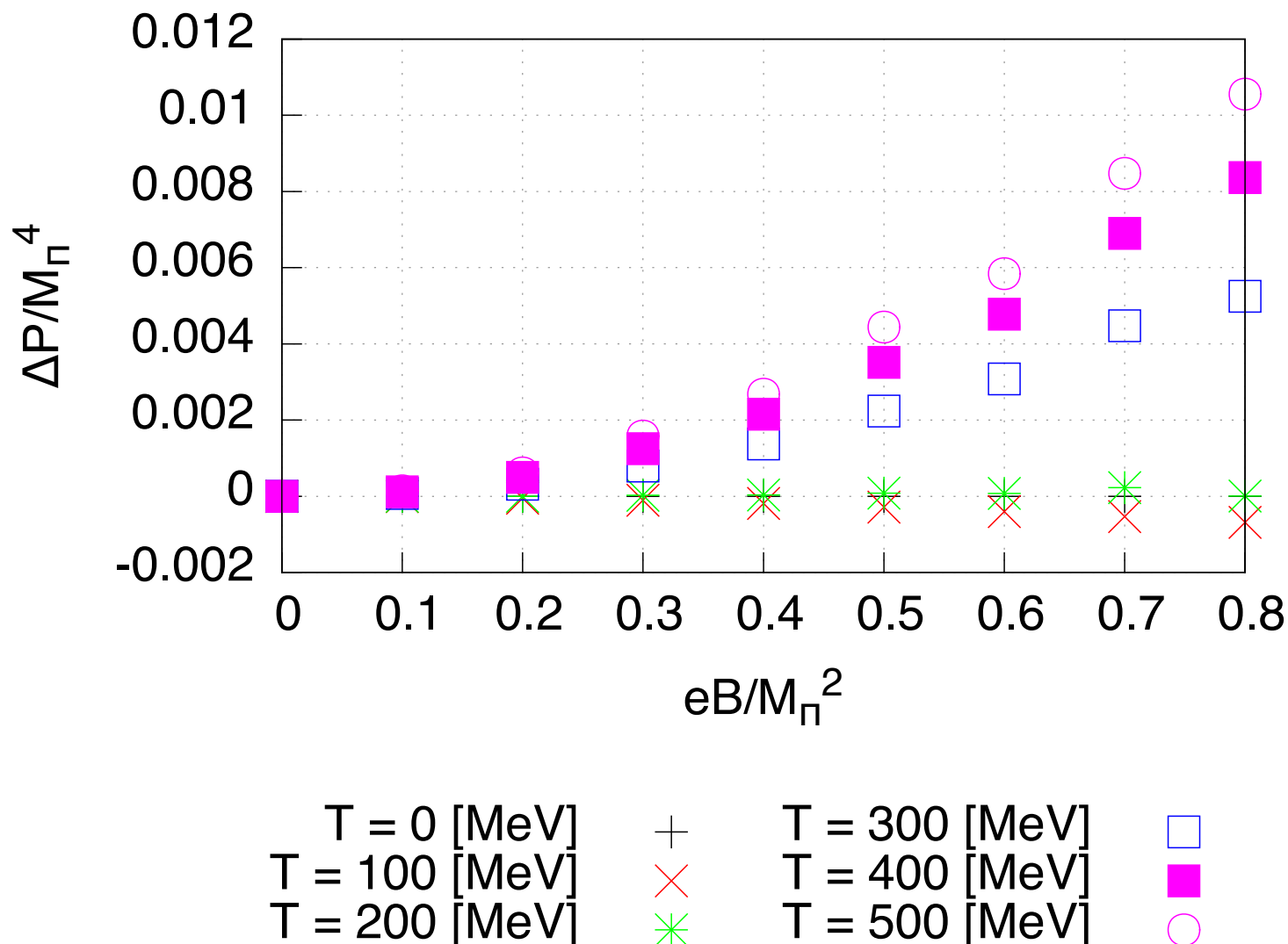
Our results



- Discrepancy between the lattice result.
- As far as we know, no chiral effective model explains the Anti-Magnetic catalyses.



Pressure



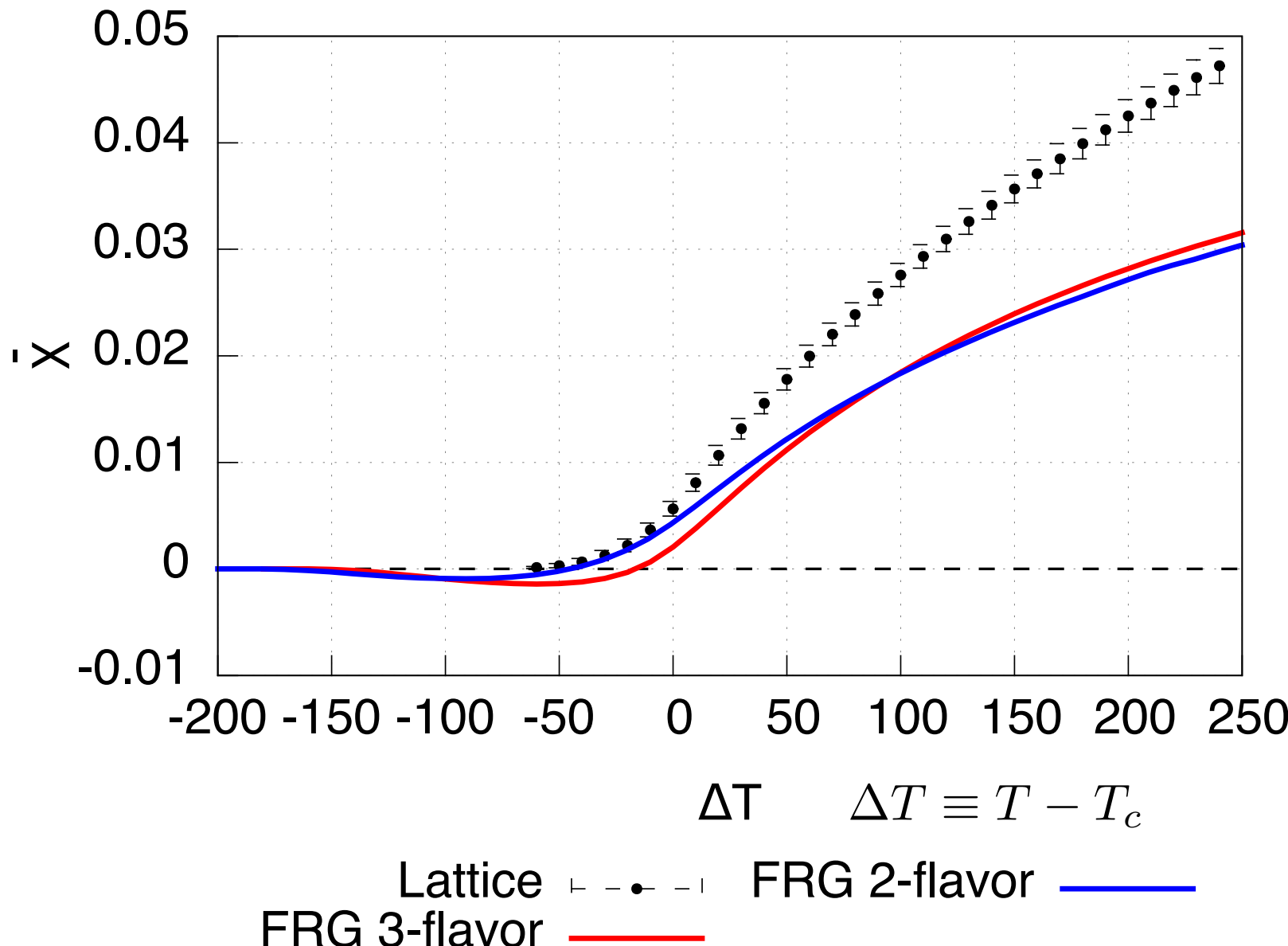
$$\Delta P(eB) \equiv (P(T, B) - P(T, 0)) - (P(B, 0) - P(0, 0))$$

- Pressure vs eB for $(0 < T < 500 \text{ [MeV]} \sim 2.5 T_c)$
- We fit the pressure with trial function using Gnuplot

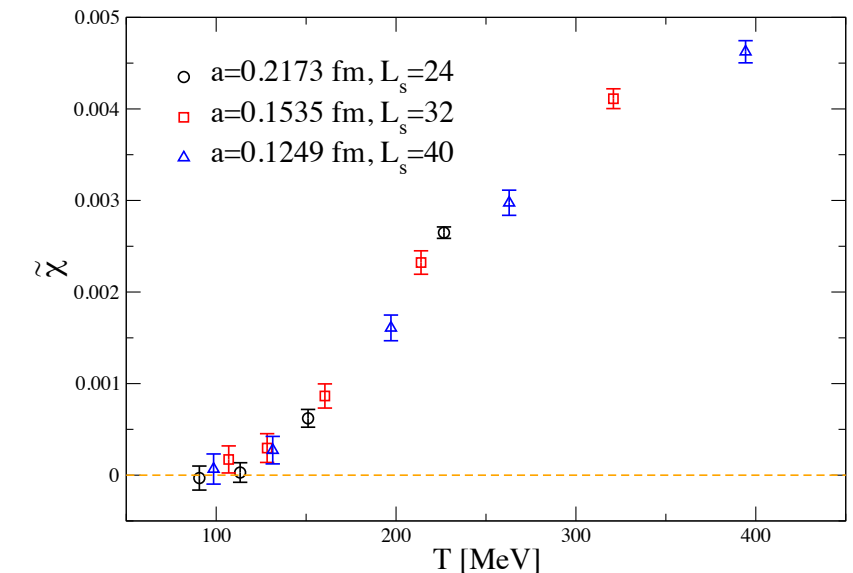
$$f(eB) = \frac{\hat{\chi}}{2}(eB)^2$$



Comparison with Lattice QCD



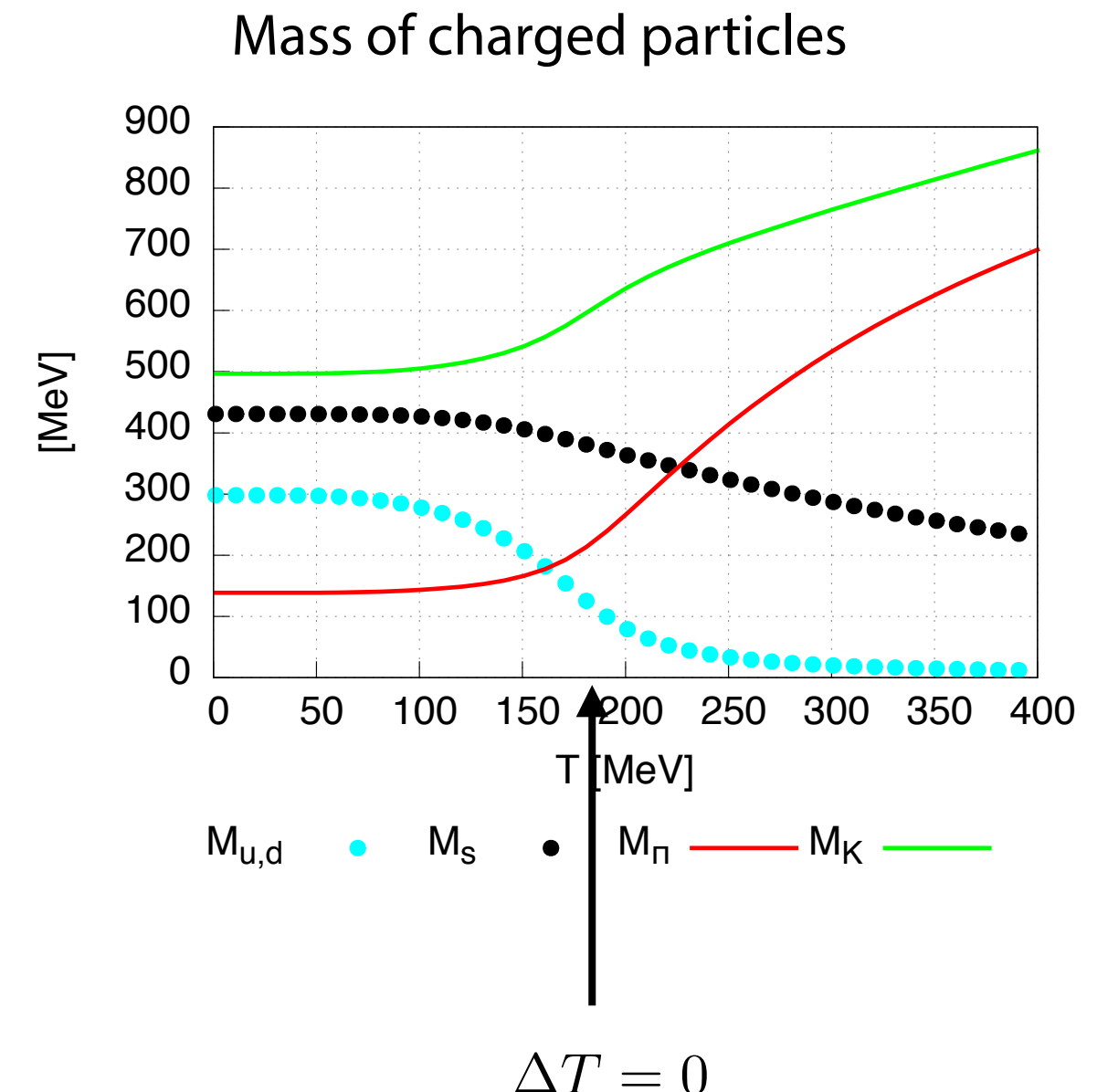
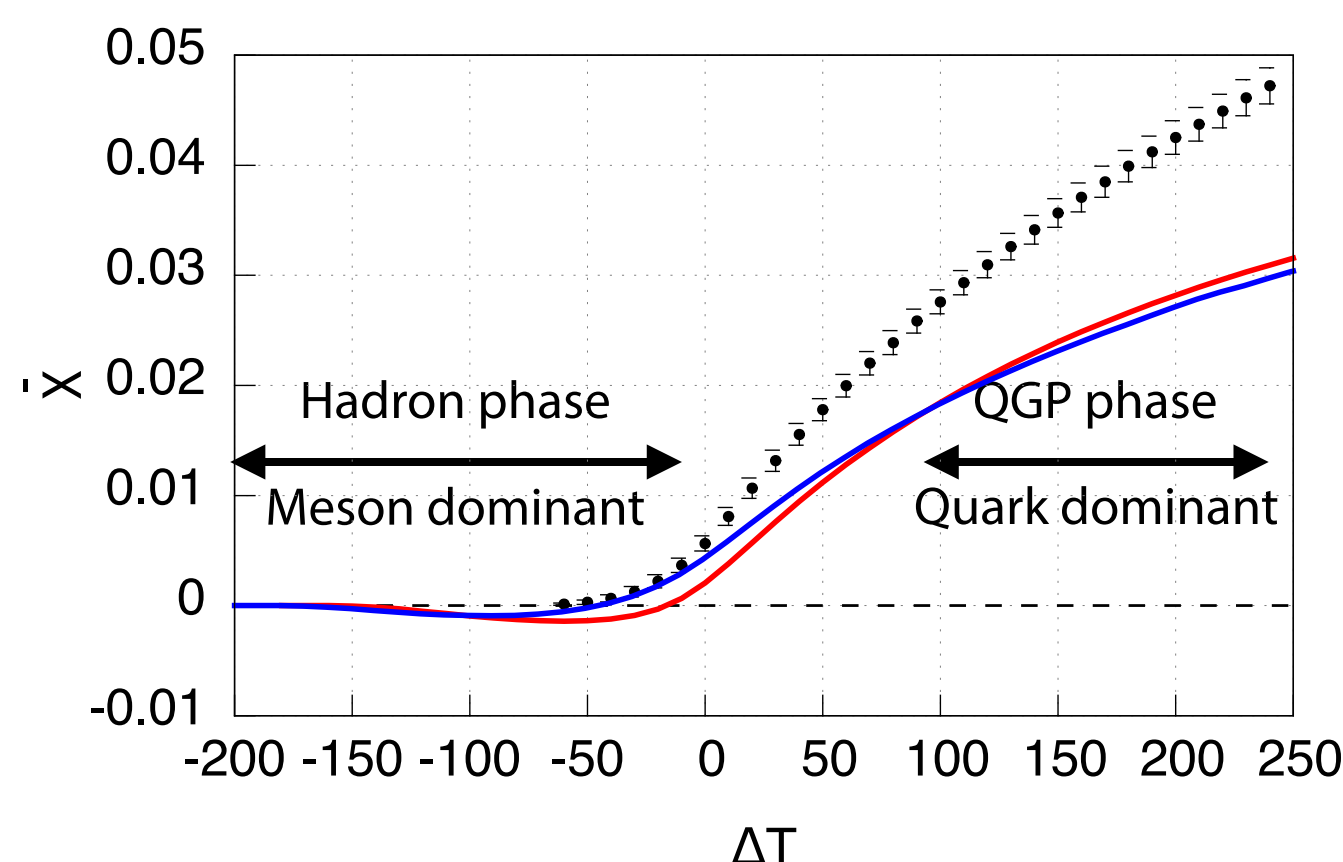
Lattice results on 2+1 flavor
Bonati et.al 2013



- At low temperature, the matter has diamagnetism.
- Near T_c , χ changes the sign and the vacuum becomes paramagnetic.



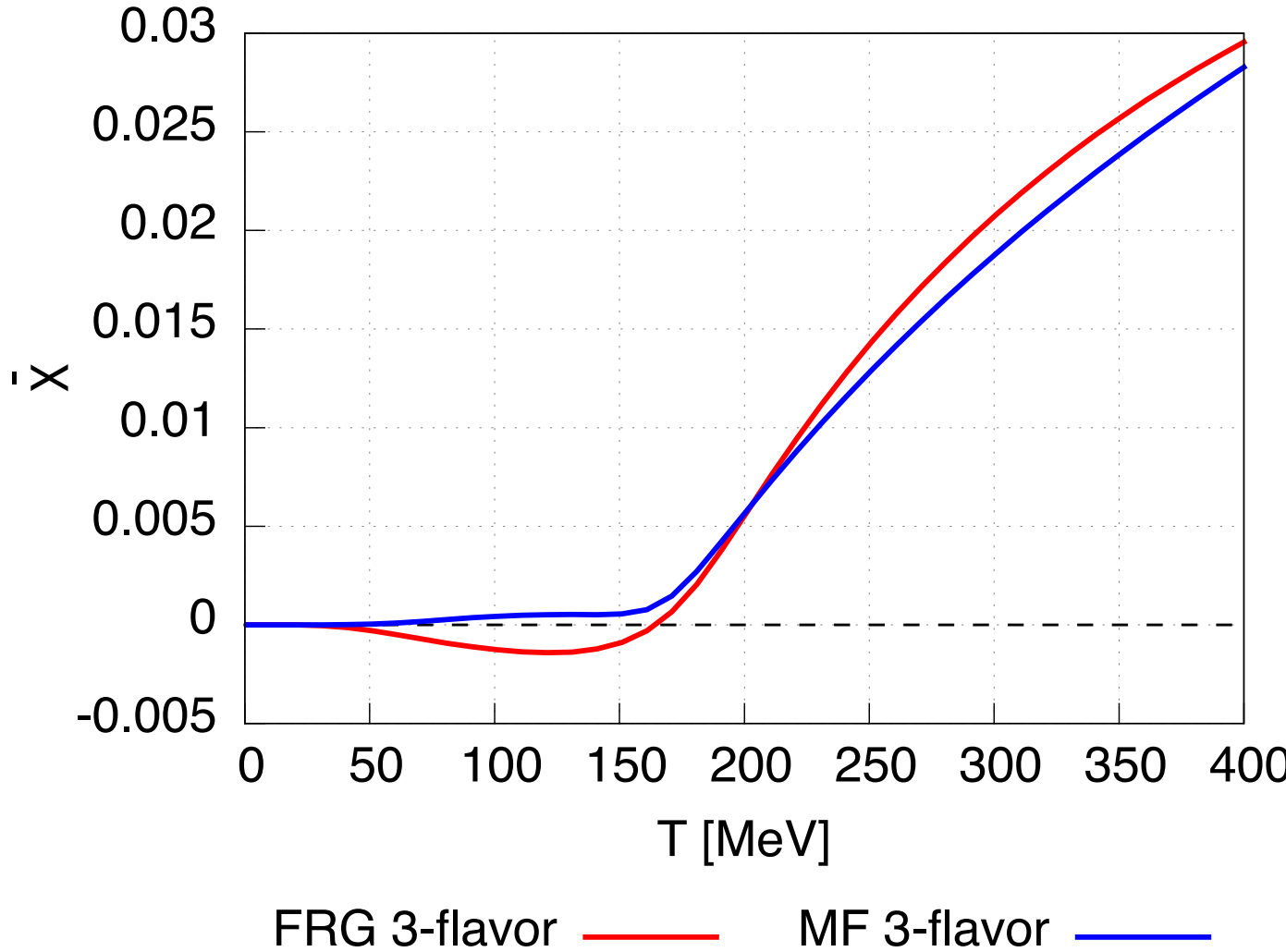
Comparison with Lattice QCD



- At Hadron phase, charged mesons (especially pion) are dominant
- While QGP phase, u,d quarks are dominant.



Mean field



$$k\partial_k \Gamma_k[\varphi] = \frac{1}{2} \text{Tr} \left[\frac{k\partial_k R_{kB}}{R_{kB} + \Gamma_k^{(0,2)}[\varphi]} \right] - \text{Tr} \left[\frac{k\partial_k R_{kF}}{R_{kF} + \Gamma_k^{(2,0)}[\varphi]} \right]$$

~~\times~~

MF: no dynamical meson

- If we neglect meson loop contributions (mean field approximation), the matter is paramagnetic at all region.
- The origin of diamagnetism is **charged mesons**.



Summary

- We solve the 3-flavor quark-meson model under strong magnetic field with Functional-RG.
- We have calculated magnetisation of the QCD vacuum at finite temperature.
- At the hadron phase, the QCD vacuum shows diamagnetism, due to light charged pions.
- At the QGP phase, the matter shows paramagnetism, due to almost bare quarks.